TIPP 2011 - Technology and Instrumentation in Particle Physics 2011

Systems-Level Characterization of Microchannel Plate Detector Assemblies, Using a Pulsed sub-Picosecond Laser

Matthew J Wetstein[a,b], Bernhard Adams[a], Matthieu Chollet[a], Preston Webster[c,1],
Zeke Insepov[a], Valentin Ivanov, Slade Jokela[a], Igor Veryovkin[a], Alex Zinovev[a], Jeffrey Elam[a], Anil
Mane[a], Qing Peng[a,2], Henry Frisch[a,b], on behalf of the LAPPD collaboration

[a]*Argonne National Laboratory*
[b]*Enrico Fermi Institute, University of Chicago*
[c]*Iowa State University*

Abstract

Microchannel plate photomultiplier tubes (MCP-PMTs) are compact imaging detectors, capable of micron-level spatial imaging and timing measurements with resolutions well below 10 picoseconds. The Large Area Picosecond Photodetector Collaboration (LAPPD) is developing techniques for fabricating 8" x 8", thin, planar, glass-body MCP-PMTs at costs comparable to traditional PMTs. Collaboration between the High Energy Physics Division and the Advanced Photon Source (APS) at Argonne National Laboratory (ANL) has produced an advanced channel-plate characterization facility for testing the time response of MCPs using a pulsed laser capable of sub-picosecond pulses. The MCPs are tested in stacks of one or two plates with a simple photocathode and coupled to a microstripline anode board. LAPPD-made MCPs have already demonstrated gains larger than 10^5 and promising time resolving capabilities. These measurements will guide the systems-level optimization of LAPPD detectors and the development of signal processing algorithms. Predictions made by the LAPPD simulations group based on electron emmission properties of the MCP pore surface are compared with these tests to help further our understanding of MCP performance.

Keywords: microchannel, MCP, characterization, photodetectors, time-of-flight, time-resolving

1. Introduction

For decades, the high energy physics (HEP) community has relied on photomultiplier tubes (PMTs) to provide low cost, large-area coverage for a wide variety of detector systems. Increasingly, the demands of HEP experiments are pushing for better spatial and temporal resolutions than PMTs can currently offer. A possible replacement for the PMT is the microchannel plate photomultiplier tube (MCP-PMT) [1], a compact detector capable of micron-level spatial imaging and timing measurements with resolutions below 10 picoseconds [2, 3, 4]. Conventional fabrication methods are too expensive for making MCPs in the
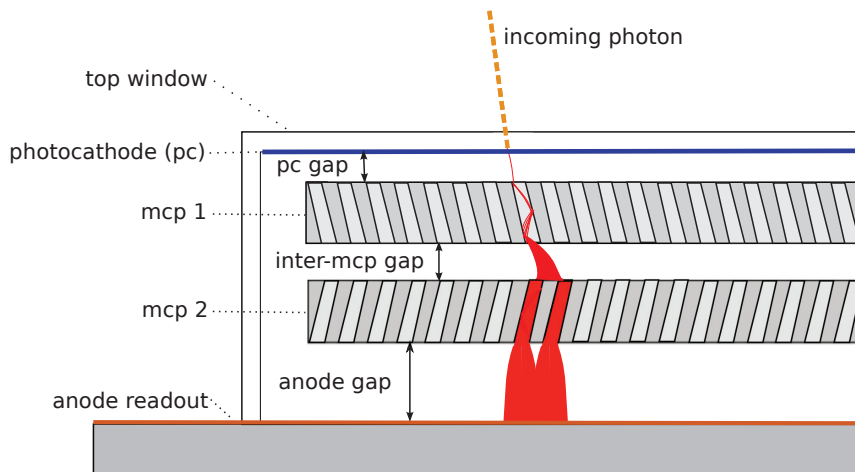
Fig. 1. The structure of a typical MCP photomultiplier tube.

quantities and sizes necessary for typical HEP applications. The Large Area Picosecond Photodetector Collaboration (LAPPD) is developing new, commercializable methods to fabricate 8" x 8" thin planar MCP-PMTs at costs comparable to those of traditional photo-multiplier tubes. The DOE funded collaboration includes 4 national laboratories, 3 companies, and 5 Universities. The project is just beginning its third year, with the goal of developing a commercializable prototype, ready for mass production. The potential for these low-cost, large-area photodetectors goes well beyond bottom-line cost reductions or merely meeting the minimal requirements of the HEP community. They are likely to enable entirely new analysis techniques.

The development of new MCP fabrication techniques necessitates a strong testing and characterization program. Several such efforts have grown out of this project at Berkeley Space Science Laboratory (SSL) [5], Argonne Material Science Division (MSD) [6], Argonne High Energy Physics Division (HEP), Argonne Energy Systems Division (ES), and the University of Chicago. This paper will focus on efforts at the Advanced Photon Source (APS) at ANL, where a dedicated laser-based laboratory has been developed for studying the timing and gain characteristics of various combinations of microchannel plates, anodes, and simple photocathodes in configurations approximating complete detector systems. With a Ti:Sapphire laser capable of pulse durations shorter than 100 femtoseconds, we are uniquely suited to study many of the timing issues at the center of this project. Furthermore, the pulsed signal can be used to assure single photon excitation for accurate gain and pulse-shape characterization, as will be discussed later in this paper. Vacuum testing chambers allow testing systems of various MCP components without the constraint of needing to seal these components in a vacuum tube.

2. Fabrication of the Microchannel Plate Detectors

Figure 1 shows the structure of a typical MCP-PMT. Light is incident on a photocathode, producing electrons by the photoelectric effect. These electrons accelerate across a potential gap toward a pair of microchannel plates, which are high-gain structures consisting of thin plates with high secondary electron emission (SEE) enhanced, microscopic pores. Voltages of roughly 1 kV are applied across each plate. Pores are typically oriented at small bias angles in opposite directions. This prevents unintended positive ions, produced in the imperfect operational vacuum, from reaching and damaging the photocathode. It also provides a well defined first strike for incoming electrons. Each electron entering a pore accelerates and strikes the pore walls, producing an avalanche of secondary electrons. The avalanche builds until the amplified pulse exits the bottom of the second MCP. This electrical signal is collected on an anode structure and passed through the vacuum assembly to front-end electronics, which digitize the signal.

Central to the project is the use of Atomic Layer Deposition (ALD) to mass produce MCPs from low cost substrates. ALD is a batch process whereby materials can be applied uniformly and conformally to large surface areas in bulk, one molecular mono-layer at a time [7, 8]. The structure of LAPPD-made MCPs is provided by inactive, porous glass discs, cut from hexagonally-packed bundles of drawn capillaries with 20 or 40 micron pore structures and corresponding 25 or 50 micron center-to-center spacing. The capilary bundles are sliced at an 8 degree bias angle to produce substrates typically 1.2 mm thick. Parameters such as the pore diameter and bias angle can have a significant impact on gain and timing characteristics, and it is possible to produce glass substrates with varying geometric properties. However, such variations go beyond the scope of our current project. The substrates are ALD coated, first with a layer of resistive material and then with a high SEE layer. This presents our effort with a unique opportunity for MCP optimization [9]. Independent control over the geometric, resistive, and SEE characteristics of MCPs enables the production of channel plates with combinations of properties not easily achievable through traditional fabrication methods. By developing and testing MCPs with a wider range of possible properties, we can place stronger constraints on models of MCP behavior.

The performance of a complete MCP detector depends not only on the channel plates themselves, but also their combinations, along with a photocathode, a particular choice of anode structure, and electronic readout. In the LAPPD design, charge from the MCPs is received by a microstripline anode structure, optimized for high-bandwidth electronics. This delay-line design greatly reduces the necessary channel count, as electronic resources scale only with the square root of the area. Hit positions are determined by the signal centroid in the direction perpendicular to the striplines, and by the difference in the arrival time at the two ends of the striplines, in the direction parallel to the strips. The electronic readout is designed to use low-cost CMOS technology. Arrival times and gains of the pulse trains are measured by waveform sampling, which offers the best timing resolution. At the ANL-APS Laboratory, we study not only the performance of the microchannel plates, but also the issues related to systems integration of these MCPs with photocathodes and various anode designs.

3. Experimental Setup

Several vacuum chambers were built to accommodate testing of 33 mm microchannel plates, and one chamber to accommodate the larger, 8"x8" format. These systems are capable of operating at vacua of the order 10^{-7} Torr. Each of these chambers has a fused silica window for transmitting UV light to MCP samples.

The MCP samples are mounted in mechanical assemblies designed to accommodate combinations of one, two, or three MCPs with a simple aluminum thin film photocathode (chosen for its robustness in air) and interchangeable delay-line anode structures. The 33 mm samples are assembled into a special, compact holder designed at Berkeley SSL, while the 8" plates are held in a custom glass tray made to match the specifications of the sealed-tube design. The spacings between the different components can be varied by swapping interchangeable, insulating spacers of different thicknesses. The voltages at each point in the MCP stacks can be independently controlled. High frequency RF cables are used to bring the signal to a multi-GHz bandwidth oscilloscope. Once the LAPPD-designed PSEC-chip [10] is available, it will be integrated into our data acquisition system.

We use a Ti:Sapphire laser to generate intense pulses of infrared light, shorter than 100 femtoseconds at a repetition rate of 1 kHz. The laser light is sent through two frequency-doubling beta-barium borate (BBO) crystals to produce UV wavelengths at around 266 nm. Currently, we are working with a beam spot of half a millimeter on the photocathode, but we plan to achieve spots sizes below 20 microns to address individual pores on the MCP. The oscilloscope trigger signal is derived from laser light incident on a fast photodiode with time jitter well below a picosecond.

4. Method

The setup described in Section 3 puts us in a position to perform accurate gain and timing measurements on the entire detection system. It also allows us to explore parameter dependencies of individual
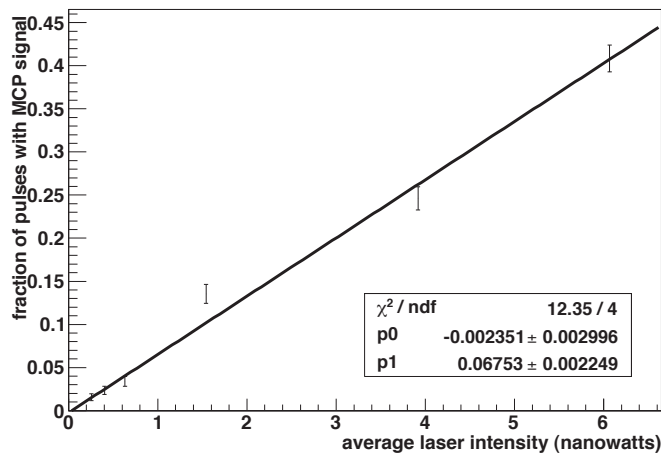
Fig. 2. Laser intensity versus the fraction of laser pulses yielding an MCP signal. Data points are fit with a straight line of slope p_1 and offset p_0.

components.

Using the laser pulses as an external trigger, we can establish the arrival time of the light pulses with accuracies better than a picosecond. This permits accurate measurement of the jitter in arrival times, the so-called "transit time spread" (TTS), even though absolute delays due to optical paths and cabling are currently only known within tens of picoseconds. Use of a pulsed laser also greatly facilitates gain measurements: by simply attenuating to the point where only a fraction f of the pulses yield a signal, we are operating in the single photoelectron regime, with the fraction f^2 being the probability of two-photoelectron events. This eliminates the need for detailed calibration of the photocathode quantum yield. Figure 2 shows the relationship between average UV intensity and the probability of a signal from a particular photocathode combined with two commercial MCPs operating in saturation mode. This high-gain MCP configuration is necessary in order to assure that the detection probability of the stack is dominated by the yield of the photocathode and not by the channel plates. Once derived, the slope in Fig 2 can be used to extrapolate to higher intensities and allow for good control over the average number of photoelectrons.

Our ability to control the size and position of the laser spot allows us to isolate particular regions of the MCP, studying their timing and gain independently. Future modifications will allow us to illuminate single pores on an MCP and send double pulses with a variable delay in order to study the recovery time of the charge-depleted regions.

5. Samples

A full series of pulsed tests were performed on a set of three MCPs, made with identical resistances, but different SEE layers. These plates were studied in two different configurations. First, we tested them as single plates, without a second MCP amplification stage. Since the signals from the lone MCPs were small, the laser intensity was set high enough to produce an average of roughly 5 photoelectrons per pulse. The readout was passed through 18 GHz, 36 dB amplifiers. Next we studied each of the ALD-based plates paired with a common commercial MCP as the second stage. The commercial plate was operated at lower than typical voltages, so that it would behave more like a linear amplifier, leaving us sensitive to gain difference between the two ALD-based plates. In both configurations, the ALD-functionalized MCPs have a thickness of 1.2 mm and a pore diameter of 20 microns. Spacing between the MCP stack and anode structure is 7mm with a gap bias of between 1 and 1.2 kV. The MCPs and the photocathode are separated by 300 micron-thick Kapton spacers with voltages varied between 100 and 400 Volts.
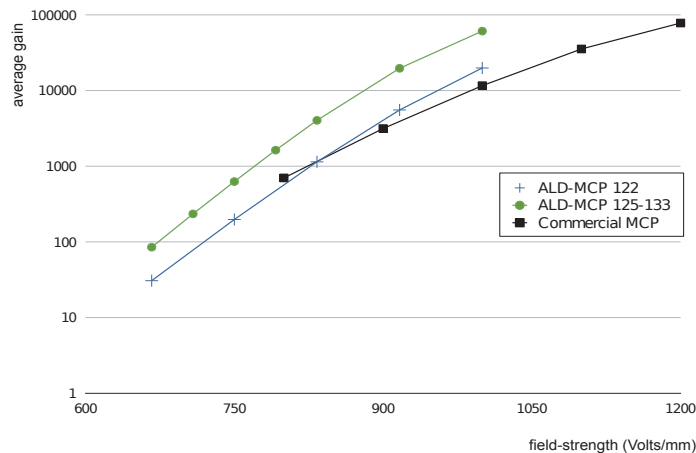
Fig. 3. Average gain curves for ALD-functionalized microchannel plates compared with the gains for a commercial MCP. ALD-MCP 125-133 refers to the average gain-voltage curve for the 8 MCPs produced in one particular batch and MCP 122 was the ALD-based channel plate with the highest observed gain measured prior to that.

6. Results

We first conducted a series of simple average gain measurements, where we determined the ratio of DC input to output currents. Typical input currents were between 10-100 picoamperes (pA), with output currents approaching a few microamperes. These efforts provide useful feedback for the construction of an average-gain characterization system by the ALD group. Single-plate gains of well above 10^4 were obtained for ALD-functionalized MCPs. These are comparable to the gains observed in a typical commercial plate. Figure 3 shows average gain comparisons of various MCPs.

Systematic tests of many different operational voltages can serve as strong constraints on models for avalanche formation in the pores. Figure 4 shows the average pulse shape for signals from a single, ALD-functionalized plate with a 20 nm MgO SEE layer, for a range of photocathode voltages. We can observe changes in both the pulse magnitude, and its arrival time. Figure 5 shows the shift in signal arrival time relative to the trigger (with optical and electronic delays included) for each photocathode voltage. Here, the signal arrival time is defined as the time when the MCP pulse crosses 50% of the pulse maximum.

Figure 6 shows the pulse height distribution for the 20nm MgO plate, with approximately 5 incident photoelectrons generated per pulse. The low-gain region of this distribution is likely shaped by experimental effects such as the dynamic range of the oscilloscope, which we are currently working on understanding.

7. Working Towards a Complete Data-Simulation Cycle

A major objective of our effort is to develop a better fundamental understanding of the relationship between material properties of the secondary electron emitter, and the avalanches that form inside the pores of an active microchannel plate. The LAPPD collaboration includes a computations and theory group developing simulations both of the material properties of our ALD coatings, and also of the avalanche formation in an MCP [11, 12]. Work is ongoing to compare these simulations with experimental results. Several MCPs were produced along with test wafers, coated with the same SEE layers, for analysis by our materials-level characterization group. The SEE properties derived from these measurements are used as inputs into the simulation group's MCP model, which is compared against experimental measurements of the corresponding MCPs.
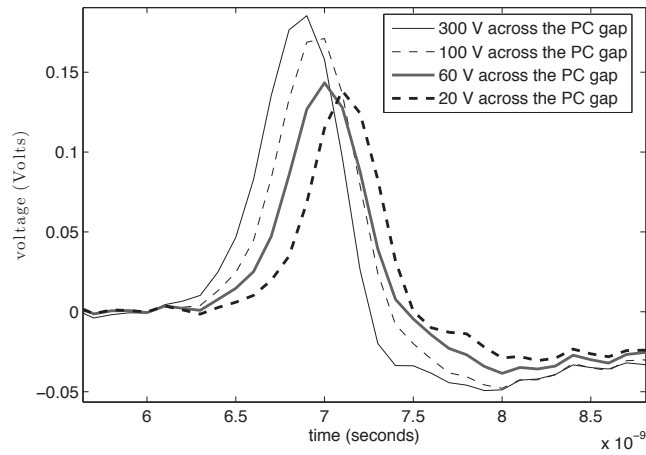
Fig. 4. Average pulse shape for signals from a 20 nm MgO coated, ALD-functionalized MCP for different applied voltages across the photocathode gap. Overshooting on the falling edge of the signal is due to the non-uniform gain/frequency characteristic of the amplfiers used.
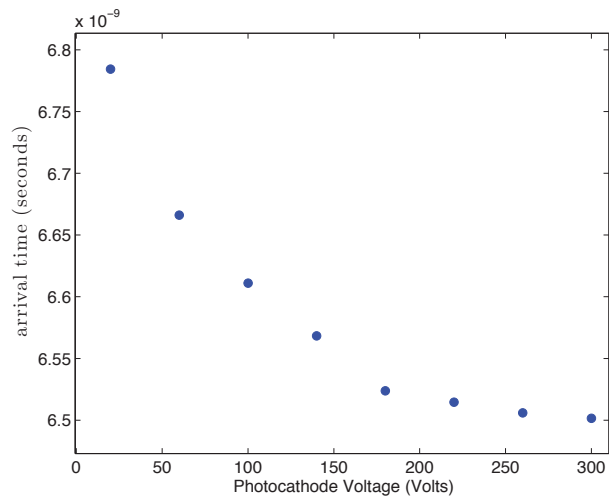

Fig. 5. Plot of the average arrival time as a function of photocathode voltage, where the arrival time is defined by a constant fraction threshold of 50%.
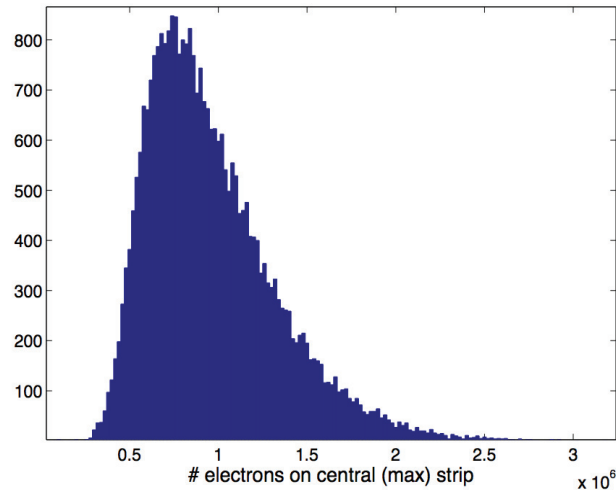
Fig. 6. Pulse Height Distribution for 20 nm MgO MCP Sample: The charge extracted per pulse (in units of elementary charge) for incident UV at an average power of 50.4 nW (around 5 incident photoelectrons per pulse).

Figure 7 shows the comparison of our best fit between the experimental pulse height distribution (in red) and the simulated distribution (in blue) for our 20 nm MgO tuning set. As discussed earlier in this paper, the lower end of the pulse height distribution is shaped by various experimental limits such as the signal-to-noise ratio, digitization of the pulses, and necessary quality cuts. However, for gains above 800,000 the simulation shows good agreements with data. Comparisons of average gains are computed for only those pulses above 800,000 electrons, in order to avoid bias.

8. 8" Testing program

Successful demonstration of working 8" x 8" microchannel plates is critical to the LAPPD effort. The ALD process is currently being re-optimized for the significantly larger active surface area of these plates. At the APS, we have completed a characterization system for testing large-format MCPs. The new testing system also enables studies of the LAPPD anode design, with 33mm MCP stacks used to produce signals incident on 8" delay-lines. Fig 8 shows some of the first pulses recorded from our full-size, transmission-line readout. The cross-talk observed along neighboring strips is expected to be much smaller in future iterations of our anode design, where spacing between the microstriplines is larger.overshoo

9. Conclusion and Future Prospects

The APS MCP characterization laboratory at Argonne has developed unique tools for studying the timing and gain characteristics of ALD-functionalized MCPs. We will continue using these tools to test detector configurations approaching a complete, final detector design. In parallel, our efforts to study ALD-based MCPs with a wide variety of electrical and SEE properties are beginning to yield new and useful data for constraining and guiding the optimization of the large area detectors. Analysis is ongoing.
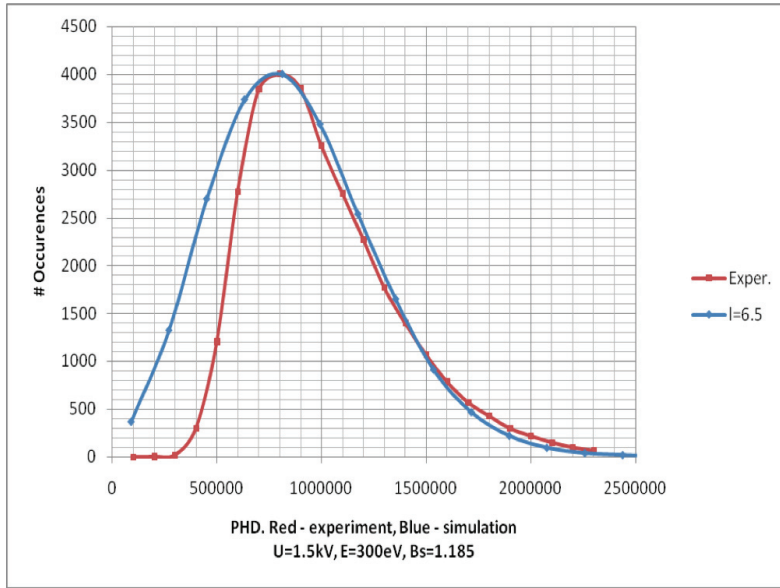
Fig. 7. Rebinned Pulse Height Distribution for a single MCP with 20 nm MgO SEE coating (from Fig 6) with simulation results overlaid.
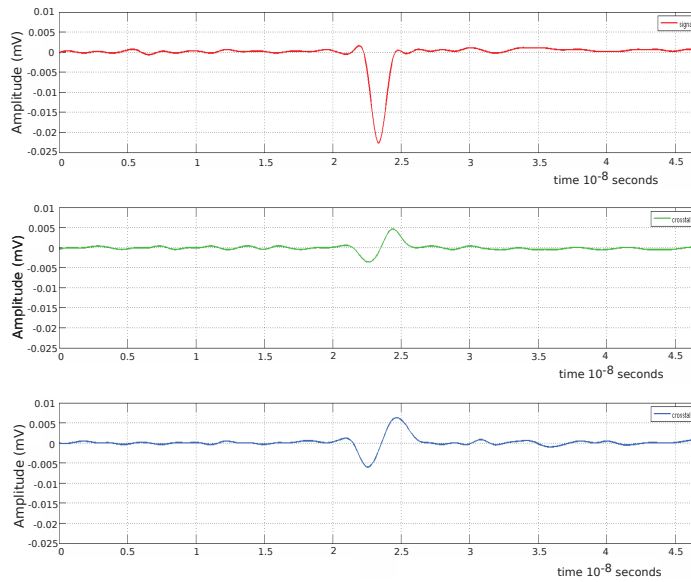

Fig. 8. Example pulses on the 8" anode, generated by a 33mm MCP stack. The top trace is the MCP signal incident on the central striplines. The lower two traces show cross-talk on the two neighboring strips. For this early test, the plates are assembled in a 33mm MCP holder, with 1 kV across each plate, 100 Volts across the 300 micron PC gap, 100 Volts across the 300 micron inter-MCP gap, and 500 V across the 1.5 mm anode gap. These parameters may change in future tests.

10. Acknowledgements

References

[1] J. L. Wiza, Microchannel plate detectors, Nucl. Instrum. Methods 162 (1979) 587–601.
[2] J. Milnes, J. Howorth, Picosecond time response of microchannel plate pmt detectors, Proc. SPIE 5580 (2005) 730–740.
[3] M. Akatsu, Y. Enari, K. Hayasaka, T. Hokuue, T. Iijima, K. Inami, K. Itoh, Y. Kawakami, et al, Mcp-pmt timing property for single photons, Nucl. Instrum. Methods A528 (2004) 763–775.
[4] K. Inami, N. Kishimoto, Y. Enari, M. Nagamine, T. Ohshima, A 5-ps tof-counter with an mcp-pmt, Nucl. Instrum. Methods A560 (2006) 303–308.
[5] O. Siegmund, K. Fujiwara, R. Hemphill, S. Jelinsky, J. McPhate, A. Tremsin, J. Vallerga, H. Frisch, J. Elam, A. Mane, D. Bennis, C. Craven, M. Deterando, J. Escolas, M. Minot, J. Renaud, Advances in microchannel plates and photocathodes for ultraviolet photon counting detectors, Proc. SPIE 8145.
[6] S. Jokela, I. Veryovkin, A. Zinovev, J. Elam, Q. Peng, , A. Mane, The characterization of secondary electron emitters for use in large area photo-detectors, Application of Accelerators in Research and Industry AIP Conf. Proc. 1336 (2011) 208–212.
[7] S. George, Atomic layer deposition: An overview, Chemical Reviews 110 (2010) 111–131.
[8] N. Sullivan, P. de Rouffignac, D. Beaulieu, A. Tremsin, K. Saadatmand, D. Gorelikov, H. Klotzsch, K. Stenton, S. Bachman, R. Toomey, Novel microchannel plate device fabricated with atomic layer deposition, Proceedings of the Ninth International Conference on Atomic Layer Deposition.
[9] J. W. Elam, S. M. George, Growth of zno/al_2o_3 alloy films using atomic layer deposition techniques, Chemistry of Materials 15 (2003) 1020–1028.
[10] E. Oberla, et al, in this proceedings.
[11] Z. Insepov, V. Ivanov, S. Jokela, et al., Comparison of secondary electron emission simulation to experimen, Nucl. Instrum. Methods A.639 (2011) 155–157.
[12] V. Ivanov, Z. Insepov, S. Antipov, Simulation of gain and timing resolution in saturated pores, Nucl. Instrum. Methods A. 639 (2011) 155–157.